Contents lists available at GrowingScience

Engineering Solid Mechanics

homepage: www.GrowingScience.com/esm

# Fly ash utilization as support of nano zinc oxide composite catalyst for methanolysis of kapok (*Ceiba Pentandra)* seed oil

**Nyoman Puspa Asri[a*], Yohannes Somawiharja[a], Yustia Wulandari Mirzayanti[b], Diah Agustina Puspitasari[c], Rachmad Ramadhan Yogaswara[d] and Jia-Ming Chern[e]**

[a]*Department of Food Technology, Universitas Ciputra Surabaya, Surabaya 60219, Indonesia*
[b]*Department of Chemical Engineering, Institut Teknologi Adhi Tama Surabaya (ITATS), Surabaya 60117, Indonesia*
[c]*Department of Chemical Engineering, Universitas Brawijaya, Malang 65145, Indonesia*
[d]*Department of Chemical Engineering, Universitas Pembangunan Nasional Veteran Jawa Timur, Surabaya 60294, Indonesia*
[e]*Department of Chemical Engineering and Biotechnology, Tatung University, 40 Chungshan North Road, 3rd Sec. Taipei, 104, Taiwan*

**ARTICLEINFO**

*Article history*:
Received 8 April 2024
Accepted 14 June 2024
Available online
14 June 2024

*Keywords*:
*Biodiesel*
*Composite catalyst*
*Coal fly ash*
*Ceiba pentranda oil*
*Zinc oxide*

**ABSTRACT**

This study focuses on developing a nano zinc oxide (ZnO) catalyst with fly ash (FA) as a support material for converting kapok seed oil (KSO) into biodiesel. This research aims to study the preparation of nano ZnO/FA solid catalysts and the catalyst's reactivity towards kapok seed oil biodiesel (KSOB) products. The catalysts were synthesized using a modification of the Stober process, which is the co-precipitation, impregnation, and precipitation step co-occurred. The catalyst is prepared on base condition using sodium hydroxide with a solvent of methanol and zinc chloride as a raw material. FA waste was effectively modified with zinc oxide particles to create a high-performance ZnO/FA composite catalyst. Under optimal stoichiometric NaOH and 60% ZnO, the resulting material achieved a remarkable specific surface area of 14.8 m²/gram, indicating its potential for enhanced catalytic activity. The prepared catalyst of nano ZnO/FA achieved successful methanolysis of KSO, with a maximum FAME yield of 61.09% attained at 65°C after 5 hours of reaction time, using a 3% catalyst dose and a KSO: methanol molar ratio of 1:15. The initial success of nano ZnO/FA with kapok seed oil paves the way for further development towards robust catalysts specifically tailored for low-grade oil conversion.



## 1. Introduction

Fossil fuel depletion and environmental pollution have urged scientific research to develop renewable and environmentally-friendly energy alternatives. Biodiesel has proven to be an energy alternative as a biofuel with significant advantages (Asri et al., 2020). Biodiesel has a low $CO_2$ and $SO_2$ level during the combustion process, better properties for engine lubrication, higher flash point, non-toxic, and high cetane number (Sharma & Singh, 2010). Another important property is that biodiesel does not require significant modification of existing diesel engines and releases less free hydrocarbon during combustion (Khan, 2020; Widjanarko et al., 2020). Biodiesel is conventionally produced via esterification and transesterification routes of edible or non-edible oils with homogenous acid or base catalysts (Sharma et al., 2010). Edible oils utilization as feedstock for biodiesel production will result in competition with food sources, and the cost of biodiesel production will increase. Therefore, many researchers developed their research on non-consumable oils. Kapok seed oil (KSO) has the potential to be the right choice to replace palm oil in Indonesia because the Indonesia State Company of Forest (PERHUTANI) is going to promote the Kapok plantation, especially in the Middle Java Province, Indonesia (Perhutani, 2022). Although homogeneous catalysts can provide high catalytic activity, some disadvantageous properties have been noted well, such as less recovery, losses of reactant due to soap formation, and the production of toxic water (Nair et al., 2012). Therefore, heterogeneous catalysts have been developed as the right solution to overcome these disadvantages. The heterogeneous catalyst has properties that are environmentally friendly, easy to separate from the reaction mixture, and reusable (Asri et al., 2020; Gurunathan & Ravi, 2015). Heterogeneous base catalysts of $CaO/\gamma\text{-}Al_2O_3$ and $CaO/KI/\gamma\text{-}Al_2O_3$ are

* Corresponding author.
E-mail addresses: nyoman.asri@ciputra.ac.id (N.P Asri)

ISSN 2291-8752 (Online) - ISSN 2291-8744 (Print)

doi: 10.5267/j.esm.2024.6.002

not suitable for LGO because of low insensitivity to free fatty acids (FFA) (Asri et al., 2015; Mandolesi et al., 2013). Heterogeneous acid catalysts can overcome these problems because they have relatively high insensitivity. The heterogeneous acid catalysts such as ZnO/γ-$Al_2O_3$ (ZA), ZnO-CuO-SO4/γ-$Al_2O_3$ (ZCSA), and ZnO/MWCNTs have developed for transesterification of kapok seed oil and kesambi oil on the previous works (Asri et al., 2018; Asri et al., 2021). However, the catalyst manufactured using γ-$Al_2O_3$ synthetic support and multi-walled carbon nanotubes (MWCNTs) is relatively expensive. Fly ash (FA) waste, which is available in abundant amounts in Indonesia, has the potential to be used as a cheap and environmentally friendly support because its chemical compositions are mainly (85%) $SiO_2$, $Al_2O_3$, and $Fe_2O_3$ (Risdanareni et al., 2017).

In this study, the authors have developed advanced materials for heterogeneous nano zinc oxide (ZnO) catalysts with FA support (ZnO/FA) to obtain a favorable catalyst with the following characteristics, e.g., large surface area, high activity, high insensitivity to FFA, robust and stable. The nano-dimensional of the solid catalysts was expected to increase the contact area between the reactants and the catalyst, so the diffusivity of the reactant would be raised (Gurunathan & Ravi, 2015). The use of FA as a supported catalyst should be very appropriate because it has many advantages, including good thermal stability, high BET performance, good dispersibility of both polar and non-polar compounds, low price, environmentally friendly, and reduced waste (Malpani & Rani, 2019; Helwani et al., 2020). The exploitation of FA-supported zinc oxide nano-heterogeneous catalyst (ZnO/FA) for KSO transesterification has yet to become well-known for recent studies. The literature investigation concluded that there is no research on ZnO/FA, nor has there been data or a kinetic model of KSO reaction with a ZnO/FA catalyst. Nano-catalysts have high activity properties because of their vast surface area, which allows the intensive contact area between the reactants, resulting in higher conversion during the transesterification reaction (Asri et al., 2021). This study aims to synthesize ZnO/FA heterogeneous catalysts with a suitable formulation for transesterifying kapok seed oil into biodiesel. Understanding the impact of NaOH quantity and ZnO loading on biodiesel yield was crucial. NaOH influences sodium methoxide formation, which is essential for making zinc methoxide (later converted to ZnO) and subsequently impacting catalyst activity. Specific ZnO/FA catalyst characteristics that led to high FAME conversion were also investigated.

## 2. Experimental and Procedure

### *2.1 Materials*

As a supported catalyst, the fly ash (FA) was purchased from an online market supplied by a coal steam-fired power plant in the East Java area. All analytical grade reagents for catalyst synthesis, such as zinc chloride, sodium hydroxide, methanol, and ethanol, were provided by Merck. Furthermore, KSO with crude grade specification was purchased from the domestic market. Each analytical laboratory supplied other analytical grade reagents for instrumentation analysis.

### *2.2 ZnO/FA catalysts preparation*

The FA was pretreated and dried at 105 °C to release moisture content. ZnO nano solid catalyst with FA as support material was synthesized using the same procedure as the previous study, which is a modified Stober process method (simultaneous impregnation and precipitation) presented by Mukenga et al. (Asri et al., 2020; Mukenga, 2012). There are some variations of catalyst preparation, viz—% loading of ZnO (from 20-60% of ZnO loading with 10% interval) as an active promotor and NaOH addition, namely 3 g and stoichiometric (around 9g) during the synthesis.

The experimental procedure to synthesize the ZnO/FA catalyst was started from $Zn(OCH_3)_2$ or zinc methoxide formation. The primary precursor, zinc chloride, or $ZnCl_2$, was reacted with sodium methoxide from an initial reaction of sodium hydroxide and methanol. Firstly, 3 grams or 9 grams of NaOH were dissolved into 100 mL of methanol to form sodium methoxide, which conformed with Eq. (1).

$$2\ Na(OH) + 2\ (CH_3OH) \rightarrow 2\ Na(OCH_3) + 2\ H_2O \quad (1)$$

Then, this sodium methoxide solution was added dropwise into the zinc chloride solution and stirred vigorously over 1 hour so that both solutions could be mixed perfectly until the precipitation of zinc methoxide occurred based on Eq. (2).

$$ZnCl_2 + 2Na(OCH_3) \rightarrow Zn\ (OCH_3)_2 + 2\ NaCl \quad (2)$$

The formed zinc methoxide particles were filtered, washed, and dried overnight at 120$^o$C. The second step was the impregnation of zinc methoxide into the surface of fly ash particles. The salt solution of zinc methoxide was made using 50 mL of ethanol as a solvent. Meanwhile, 10 grams of fly ash were dissolved into 50 mL aquadest. After that, the zinc methoxide solution was wisely dropped into the FA mixture at 70$^o$C for 1 hour, followed by further evaporation until the solution transformed into a slurry. The final slurry, subsequently, was dried overnight to release the rest of its moisture content. The dried solid catalyst was crushed and calcined at 500$^o$C under airflow for 5 hours to form the nano ZnO/FA catalyst. The calcination reaction to convert zinc methoxide as a salt into its oxide form (ZnO) is shown in Eq. (3).

$$2\ Zn(OCH_3)_2 \rightarrow 2\ ZnO + 2\ CH_3O + 3H_2 \quad (3)$$

Afterward, the FA and prepared ZnO/FA solid catalyst were characterized using several techniques like X-Ray Diffraction (XRD) analysis to study the crystal structure and nitrogen ($N_2$) adsorption-desorption followed by mathematical calculation using Brunauer Emmet Teller (BET) formula for the solid nanoparticle surface area measurement. The other characterization was scanning electron microscopy (SEM), which studied the surface morphology of the nanoparticle and X-ray fluorescence (XRF) to determine crystalline elements more specifically and quantitatively inside the solid catalyst material. Moreover, the ZnO/FA solid catalyst was also analyzed using Fourier-transform infrared spectroscopy (FTIR) analysis to measure the functional groups that play an essential role in building the chemical structure of the ZnO/FA catalyst.

*2.3 ZnO/FA catalysts activity analysis*

The ZnO/FA catalyst reactivity was analyzed for converting kapok seed (*Ceiba pentandra*) oil (KSO) into biodiesel via transesterification in a batch process. This raw material is a lower-grade oil with impurities like gum and free fatty acids. Before the transesterification reaction, kapok seed oil (KSO) undergoes a crucial degumming process. This specific treatment, described in detail by Putri et al., 2012, effectively removes gum and other contaminants from the oil, ensuring its readiness for the subsequent chemical conversion. Notably, the degumming procedure used here remains unchanged from our previous work (Asri et al., 2020).

The treated kapok seed oil was transesterified in a 250 mL flask reactor setup to produce biodiesel using prepared ZnO/FA catalyst, which is synthesized involved the variation of NaOH edition (3 g and stoichiometrically) and ZnO loading (20, 30; 40; 50 and 60% (wt. % into FA)). The reaction temperature for the transesterification was 65°C, while the catalyst concentration was kept at 3%. Additionally, a 1:15 molar ratio of KSO to methanol was employed. The complete procedure refers to previous research (Asri, et al., 2020; Asri et al., 2022). The calculation of the yield of kapok seed biodiesel (KSOB) was performed using Eq. (4),

$$Yiel\ KSOB\ (\%) = \frac{mass\ KSOB}{mass\ treated\ KSO} \times 100 \quad (4)$$

Some parameters to investigate the quality of kapok seed oil biodiesel (KSOB) quality are density, viscosity, FFA content, moisture content, and saponification value. FFA content was analyzed using a titration technique with a base solution. In this work, NaOH solution was used as a base titer, and the FFA content was measured using Eq. (5),

$$\%FFA = \frac{\text{volume of titer} \times \text{molarity of NaOH} \times 28}{\text{mass of sample}} \times 100\% \quad (5)$$

Saponification values (SV) were also measured via titration using a phenolphthalein indicator. HCl was utilized as an acid solution on the titer side, and this value was calculated using Eq. (6),

$$SV = \frac{\text{volume of titer} \times \text{molarity of HCl} \times 56.1}{\text{sample weight}} \quad (6)$$

## 3. Results and discussion

*3.1 Fly ash characteristics*

X-ray diffraction (XRD) analysis of FA was conducted using Bruker D8 Advance X-ray diffractometer with Cu K-α (λ = 1.54 Å), as shown in **Fig. 1**. The FA particles revealed the highest peak at 26.5° and can be indexed to the quartz crystal structure (ICDD: 000-46-1045) (Katara et al., 2020). Furthermore, other appearances were not intense, and sharp peaks on angle 2θ range from 33° to 35°. These peaks are related to ICDD standard reference 000-47-1743 for $CaCO_3$ in the form of calcite and ICDD 000-33-0664 for $Fe_2O_3$ as a hematite (Widayat et al., 2017). While XRD analysis might reveal a peak seemingly similar to pure aluminum (JCPDS 000-04-0787), as reported by Asri et al., 2020, its broad, uncharacteristic shape suggests the presence of an amorphous phase rather than crystalline aluminum. This implies that the material analyzed lacks the defined atomic arrangement of pure aluminum.

XRF characterization confirms these findings, revealing that over 92.2% of Fly ash (FA) is mainly composed of four minerals: silica ($SiO_2$), iron oxide ($Fe_2O_3$), calcium oxide (CaO), and aluminum oxide ($Al_2O_3$). As shown in **Table 1**, silica makes up the largest portion at 30.7%, followed by iron (III) oxide at 27.0%, calcium oxide at 23.5%, and aluminum oxide at 11%. However, this composition can vary significantly depending on the source of the raw materials and the operating conditions of the coal-fired boiler. For instance, Katara et al. (2020) reported a fly ash with a much higher silica content (59.42%wt). This highlights the importance of considering the specific source and production process when characterizing fly ash for potential applications.

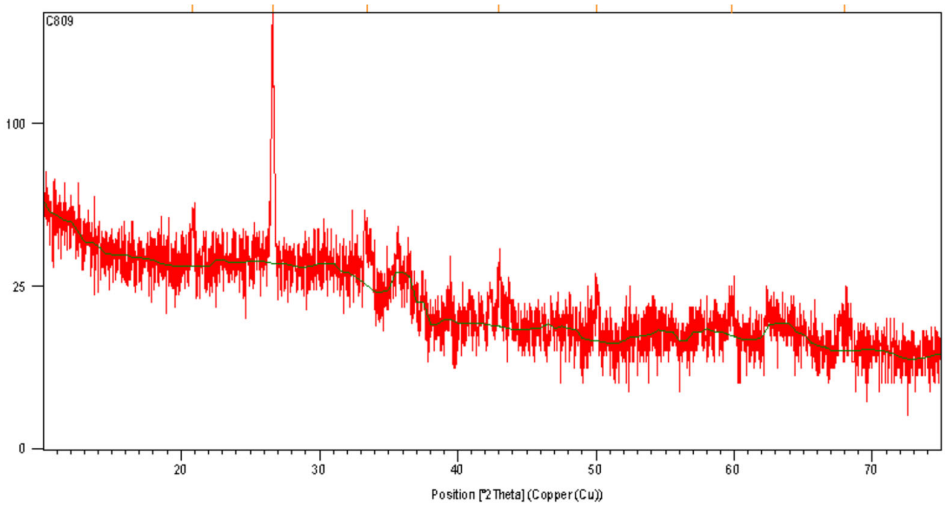


**Fig. 1**. Fly ash X-ray diffraction

**Table 1.** Composition of oxide compounds and elements of fly ash from XRF analysis

| No | Oxide compound | Composition (%wt) | Compound | Composition (%wt) |
|---|---|---|---|---|
| 1 | $Al_2O_3$ | 11 | Al | 8.4 |
| 2 | $SiO_2$ | 30.7 | Si | 20.5 |
| 3 | $SO_3$ | 0.3 | S | 0.2 |
| 4 | $K_2O$ | 1.59 | K | 2.08 |
| 5 | CaO | 23.5 | Ca | 27.4 |
| 6 | $TiO_2$ | 1.54 | Ti | 1.59 |
| 7 | $V_2O_5$ | 0.05 | V | 0.05 |
| 8 | $Cr_2O_3$ | 0.094 | Cr | 0.11 |
| 9 | MnO | 0.35 | Mn | 0.49 |
| 10 | $Fe_2O_3$ | 27.0 | Fe | 34.5 |
| 11 | NiO | 0.056 | Ni | 0.087 |
| 12 | CuO | 0.054 | Cu | 0.084 |
| 13 | ZnO | 0.03 | Zn | 0.05 |
| 14 | SrO | 0.78 | Sr | 1.3 |
| 15 | $ZrO_2$ | 0.2 | Zr | 0.2 |
| 16 | $MoO_3$ | 1.3 | Mo | 1.3 |
| 17 | BaO | 0.47 | Ba | 0.73 |
| 18 | $Eu_2O_3$ | 0.33 | Eu | 0.51 |
| 19 | $Yb_2O_3$ | 0.01 | Yb | 0.01 |
| 20 | $Re_2O_7$ | 0.1 | Re | 0.2 |
| 21 | HgO | 0.16 | Hg | 0.29 |

Surface area of FA was determined by Nitrogen ($N_2$) adsorption–desorption characterization followed by mathematical calculation of surface area using Brunauer Emmet Teller (BET) formula. The surface area is obtained through a slope of 51340.512 and an intercept of -4660 on the BET multi-point plot, and found 0.075 $m^2$/gram as shown in **Fig. 2**. The resulting surface area is smaller compared to previous studies by Katara et al., which reached 9.18 $m^2$/gram (Katara et al., 2020). However, this specific surface area obtained in this study is still within the same range as the FA characteristics shown by Babajide et al., below 1 $m^2$/gram (Babajide et al., 2010). The characteristics of FA particles, which have a small surface area, are justified by their surface morphology, which is perfectly spherical based on scanning electron microscopy (SEM) analysis.

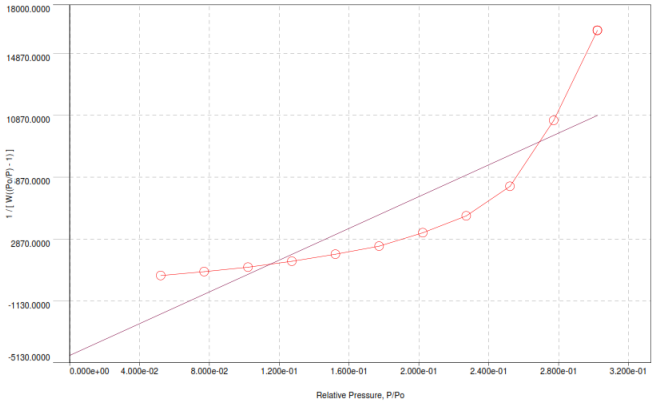


**Fig. 2**. BET multi-point of fly ash

The morphological surface of FA from the SEM image (**Fig. 3**) showed that its shape is spherical and dense. The morphological form of the FA does not show significant pores and tends to have a crystalline structure. This crystalline morphology is consistent with the XRD results, which show the peaks of $SiO_2$ quartz crystals. The FA morphological shape conforms to the results obtained by Katara et al., which showed perfectly spherical particles with a smooth outer surface (Katara et al., 2020). The FA particle morphology appeared due to its formation from heating at high temperatures in a boiler combustion furnace and further suddenly cooled before being deposited in the ash yard (He et al., 2019). SEM analysis can also predict the particle size of FA by measuring its diameter. The diameter of FA that can be measured through SEM images due to the characterization is in the range of 5 – 30 μm. This FA particle size is smaller than the results published by Babajide et al., which is in the diameter range of approximately 30 – 100 μm (Babajide et al., 2012).

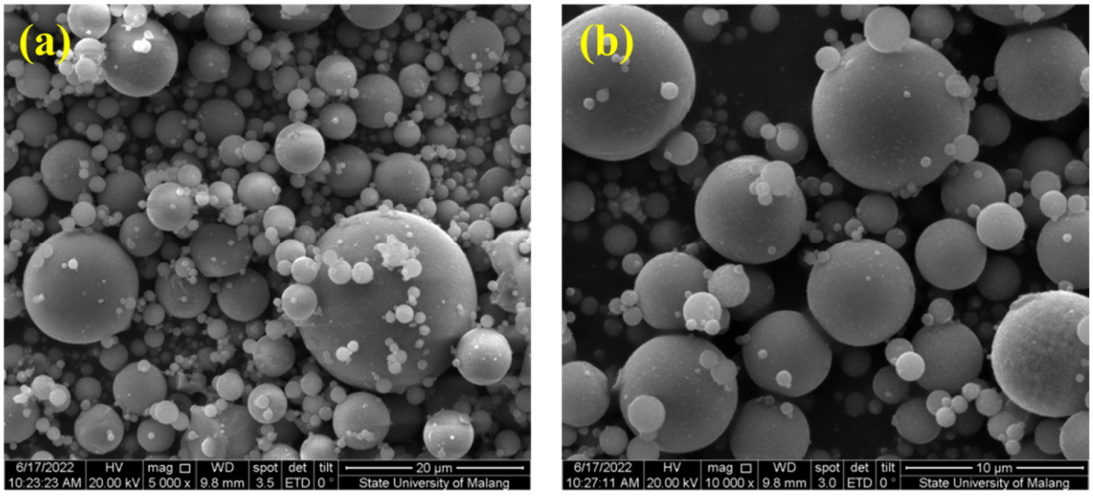


**Fig. 3**. SEM images of fly ash for various magnifications: (a) 5000x; (b) 10,000x

*3.2 ZnO/FA solid catalyst characteristics*

The specific area of raw FA was found to be very low at 0.075 $m^2$/gram, and by thermal treatment and impregnation with ZnO, after the calcination process at 500°C the BET surface area significantly increased to 14.8 $m^2$/gram. These results are lower than those obtained in the study of Yusuf et al., which obtained a surface area of 58.76 $m^2$/g by calcination at 400°C (Yusuff et al., 2021). The initial treatment of FA with HCl and then the calcination temperature seemed to affect the surface area of the catalyst to be obtained considering the research of Yusuf et al., which used 500ºC of temperature and also produced almost the same surface area of 16.62 $m^2$/g (Yusuff et al., 2021). These findings indicate that at higher temperatures (500°C), a change in crystallization phase and sintering occurs with increasing calcination temperature, reducing surface area. Al Sharifi and Znad reported similar observations in the methanolysis of Canola oil on lithium-based chicken bones, where the composite catalyst's thermal treatment at high temperature reduced surface area (AlSharifi & Znad, 2019).

XRD analysis was also used to detect the presence of ZnO particles as a promoter on the FA surface as a catalyst support (**Fig. 4**). The detection can be seen from the diffraction peaks, which are the same as the ZnO diffractogram pattern standard. The dispersed ZnO on the FA surface acts as an active site and increases the activity of the catalyst (Yusuff et al., 2021). The characterization results confirm that ZnO has been dispersed on the FA surface based on the peak reference of ZnO and FA. The peak reference of the ZnO diffractogram is given by JCPDS (Joint Committee of Powder Diffraction Standard) 00-036-1451 with a peak of 2θ angle of 31.4; 33.8; 35.8; 46.8; 55.9; 61.7; 65.5; 66.9; 68.2 degrees. This XRD pattern shows the wurtzite structure of ZnO and seems to have a more crystalline structure (Asri et al., 2021). Increased dispersion of ZnO particles on FA leads to a sharper peak in the ZnO diffractogram, suggesting a more crystalline structure (Istadi et al., 2015). This trend aligns with observations from previous studies using different support materials like γ-$Al_2O_3$ and carbon nanotubes (Asri et al., 2018, 2021). In line with the XRF analysis in **Table 2**, where higher ZnO loadings directly correlate with increased zinc oxide composition in the ZnO/FA catalyst. For instance, a 20% (%wt. to FA) ZnO loading corresponds to a 42.70% zinc oxide composition, while a 50% loading boosts it to 59.10%. This further substantiates the link between dispersed ZnO particles on the FA surface and the resulting crystallinity of the catalyst. The influence of NaOH addition on ZnO is evident in both the XRD diffractogram (**Fig. 4**) and XRF analysis (**Table 2**). At 50% ZnO loading, the ZnO peak exhibits significantly higher sharpness with stoichiometric NaOH addition compared to 3g NaOH. This observation aligns with the XRF results, where stoichiometric NaOH addition led to a higher ZnO composition (59.10%) compared to 3g NaOH (49.8%). The disparity in ZnO content is readily explained by considering the reaction mechanism (equations 1, 2, and 3). Adding stoichiometric NaOH (9g) leads to the formation of a larger amount of sodium methoxide intermediate. This, in turn, reacts with zinc chloride to produce zinc methoxide, which ultimately decomposes into zinc oxide during the calcination process. This sequence

effectively translates the added NaOH into more ZnO, accounting for the higher observed composition, potentially contributing to the observed variation in peak sharpness and suggesting an impact on crystallinity.

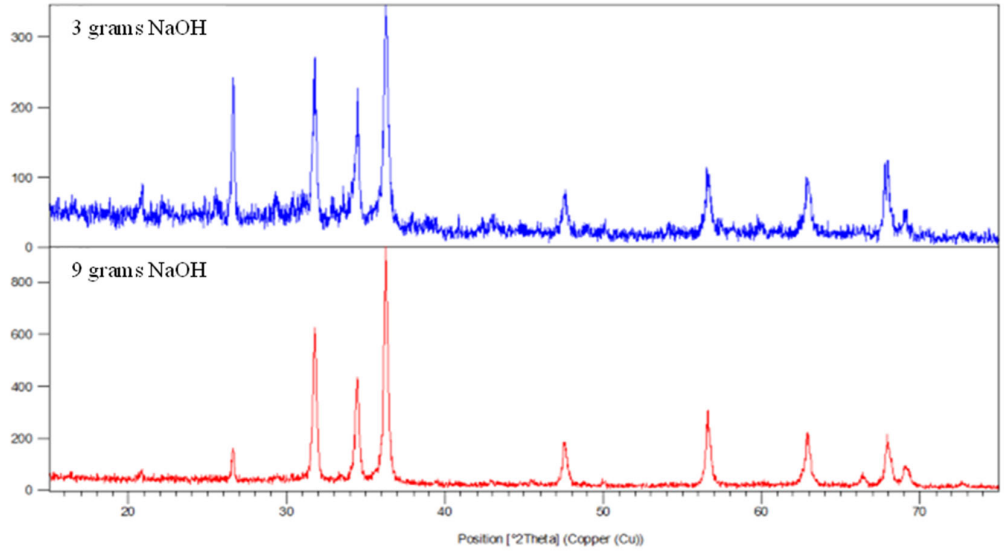


**Fig. 4**. XRD result of Zn/FA solid catalyst with 50% ZnO loading and the addition of 3 and 9 grams of NaOH

**Table 2.** Comparison of major oxide compositions in ZnO/FA Catalyst at 20% and 50% ZnO loading with 3 g and stoichiometric NaOH addition (XRF)

| ZnO loading %)/NaOH addition | Oxide Compound (%) | | | | | |
|---|---|---|---|---|---|---|
| | $Al_2O_3$ | $SiO_2$ | CaO | $Fe_2O_3$ | ZnO | Others (trace element) |
| 20/ stoichiometrically | 6.50 | 20.00 | 12.70 | 14.20 | 42.70 | 3.90 |
| 20/3 g | 9.70 | 25.9 | 18.3 | 18 | 21.50 | 6.60 |
| 50/ stoichiometrically NaOH addition | 3.2 | 8.6 | 5.95 | 7.26 | 59.10 | 15.89 |
| 50 / 3g | 5.8 | 16 | 11.5 | 13 | 49.8 | 3.9 |

We also examined the morphology of the prepared ZnO/FA catalyst using the same methods and equipment as those employed for the FA analysis, specifically scanning electron microscopy (SEM). **Fig. 5** reveals the altered morphology of the ZnO/FA catalyst compared to the original, unaltered FA (which exhibited round and solid shapes) (**Fig. 3**). Notably, white flower-like particles now decorate the FA surface, indicating the successful dopp dispersed of ZnO onto the FA support. Fig. 4's XRD analysis confirms this evidence, by the appearance of some distinct peaks of ZnO characteristic of the material. Furthermore, peaks corresponding to $SiO_2$ (the primary component of fly ash) and $Fe_2O_3$ (identified as $ZnFe_2O_4$ at 2θ of 56.7°) are also present. This indicates the incorporation of both ZnO and $Fe_2O_3$ (potentially merged as $ZnFe_2O_4$) from the fly ash, corroborated by the compositional data of ZnO/FA found in the XRF analysis (**Table 2**).

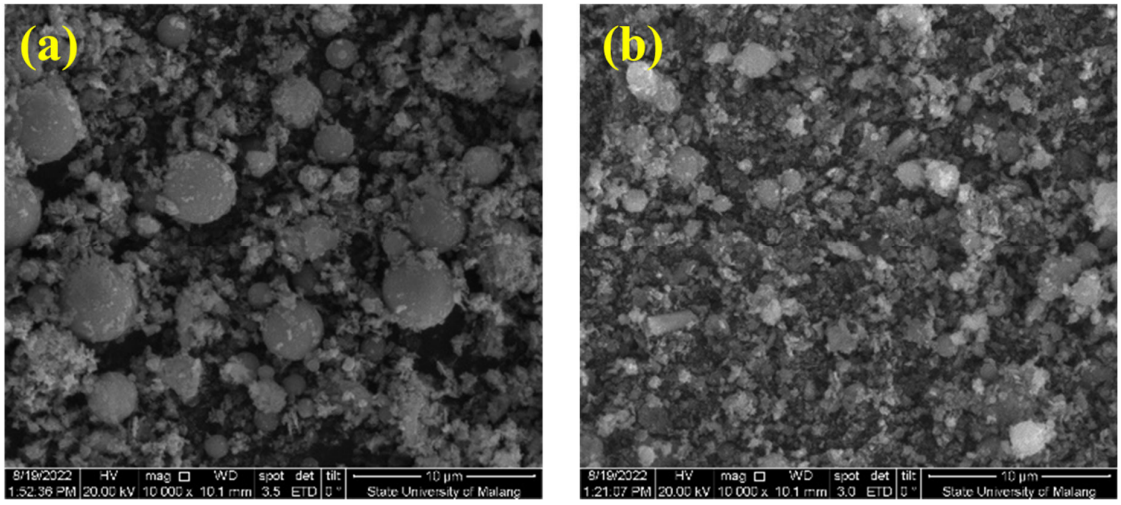


**Fig. 5**. SEM images of ZnO-FA for magnifications 10,000X; (a) NaOH addition (3 g): b) NaOH addition (stoichiometry)

The FTIR spectrum of the ZnO/FA catalyst samples loaded with 50% ZnO against FA reveals several functional groups associated with each sample as shown in Fig. 6. The wavenumber at about 3500 $cm^{-1}$ in all materials is related to the stretching vibration O-H mode of the water molecules closely similar to the oxide catalyst that Roy et al. reports showed 3740 $cm^{-1}$ of peak characteristic indicating O-H symmetric stretching (Roy & Sharma, 2020). Also, a peak at around 2380 $cm^{-1}$, which corresponds to C-H asymmetric/asymmetric stretching, was detected in the ZnO/FA catalyst samples (Yusuff & Bello, 2019). The sharp peak observed at 1400 $cm^{-1}$ in the ZnO/FA sample is associated with the O-Si-O asymmetric stretching mode, similar to that reported by Yusuff et al. (Yussuf et al., 2019). Meanwhile, the appearance of bands at 883 and 933 $cm^{-1}$ in the ZnO/FA sample was caused by out-of-plane Al-O vibrations, and ZnO/FA showed a peak at 883 $cm^{-1}$, which can be ascribed to Al-Mg-OH vibrations (Olutoye & Hameed, 2011). Undoubtedly, the functional groups detected on the surface of this ZnO/FA composite significantly affect the catalytic reaction.

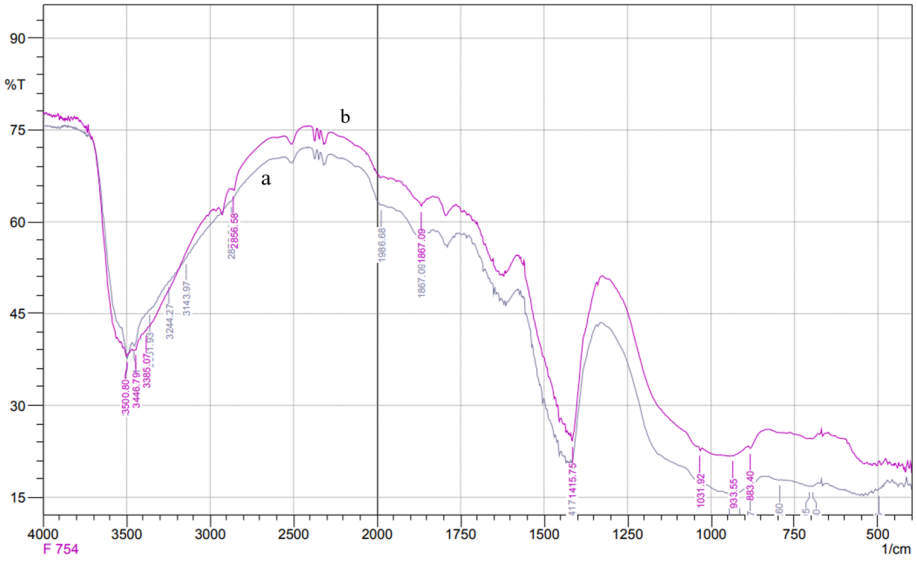


**Fig. 6**. FTIR analysis result curve of ZnO/FA catalyst for 50% ZnO loading

*3.3 ZnO/FA solid catalyst activity analysis*

The synthesized ZnO/FA catalysts were tested through the KSO transesterification process under methanol reflux conditions (65ºC of reaction temperature), reaction time of 3 hours, catalyst dose of 3 %wt., molar ratio of KSO to methanol 1:15 to determine their activity of the ZnO/FA catalyst. The amount of zinc oxide (ZnO) loaded onto the catalyst significantly impacted the resulting yield of kapok seed oil biodiesel (KSOB), as illustrated in **Fig. 7**. Yields were lowest at 20% ZnO loading, reaching only 26.44% and 28.85% with 3 g and stoichiometric (9 g) NaOH addition, respectively. This suggests insufficient ZnO initially limited the reaction, leading to an incomplete conversion and lower yield. In contrast, the highest yields of 57.01% and 64.09% were achieved at 60% ZnO loading with 3 g and stoichiometrically NaOH addition, respectively. The dramatic increase in KSOB yield observed with increasing ZnO loading (**Fig. 3**) suggests that ZnO plays a critical role in promoting catalytic activity. This likely involves enhanced surface area for reactant adsorption, potentially leading to improved reaction kinetics and efficiency. This clear trend demonstrates the crucial role of ZnO as a promoter in boosting catalytic activity. Further investigation is needed to elucidate the specific mechanisms underlying this promotional effect.

Many factors affect the transesterification process, including not only the type and quality of triglyceride (TG) but also the type and route of catalyst synthesizing. Likewise, the type of support and promoter of the catalyst plays a significant role in increasing the activity of the catalyst (Asri et al., 2013). In addition, the transesterification process variables such as reaction temperature, reaction time, molar ratio of oil to methanol, catalyst dose, and stirring speed also significantly affect the quality and quantity of biodiesel produced (Asri et al., 2013). Yusuff et al. also stated the highest yield of 83.17 %wt. and the FAME content of 98.14 %wt. that was achieved at the optimum temperature of 140°C, 3 hours of time reaction, methanol/oil molar ratio of 12:1 and catalyst loading of 0.5 %wt. (Yussuf et al., 2021). Another researcher also reported the maximum oil conversion of 86.13 % that was achieved on transesterification of sunflower oil using a fly ash-based catalyst loaded with 5% wt. of $KNO_3$ at a reaction temperature of 160ºC, the reaction time of 5 hours and a methanol/oil ratio of 15:1, and 15 %wt. of catalyst dose (Babajide et al., 2012).

Our study achieved a lower biodiesel yield compared to previous works (Yusuf et al. 2021; Babajide et al., 2012). This can be attributed to several factors. Firstly, our transesterification temperature (80°C) was significantly lower than theirs (150°C and 160°C, respectively). Secondly, Yusuf et al. (2021) pretreated their fly ash and used waste cooking oil with low free fatty acids (FFA), while we used untreated FA and kapok seed oil with high FFA (10%). Babajide et al. (2012) used

soybean oil with lower FFA. However, we identified a potential route to improve catalyst activity. By modifying the fly ash synthesis to include pretreatment and functionalization with sulfonate groups, we could mimic the approach of Yusuf et al. and potentially achieve higher performance. These modifications enhance the surface area of the fly ash, allowing zinc oxide (ZnO) to adhere more effectively (Yusuf et al., 2021; Muñoz et al., 2020).

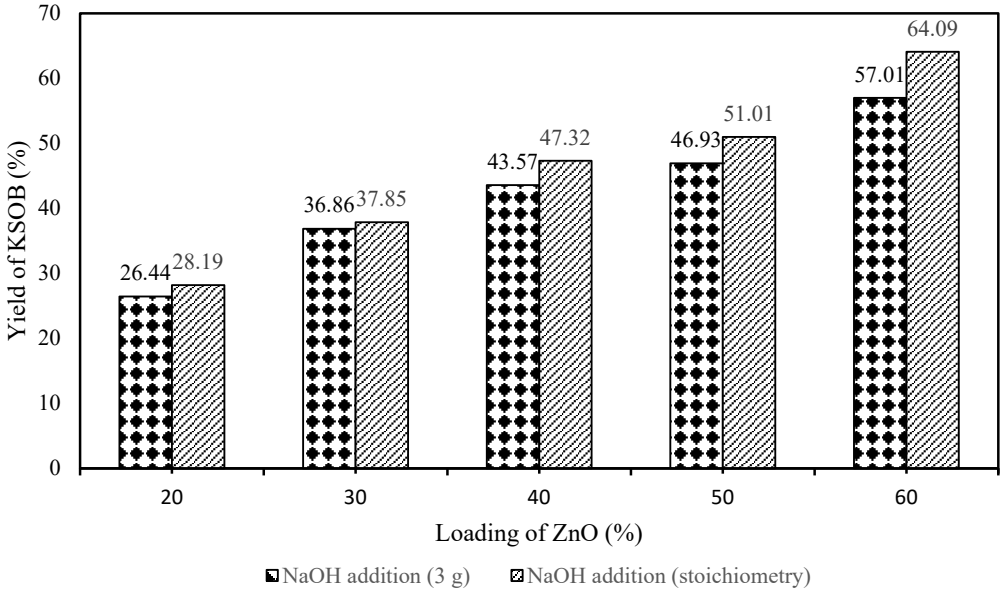


**Fig. 7**. Effect of NaOH addition and ZnO loading on biodiesel yield

*3.4 KSOB characteristics*

Biodiesel from the transesterification of Kapok seed oil (KSOB) was characterized, including density, moisture content, free fatty acids (FFA as oleic acid), viscosity, and iodine value. **Table 3** shows the properties of biodiesel resulting from this work compared to the biodiesel standard according to SNI 7182-2015. These results indicate that the characteristics of the biodiesel produced almost follow the SNI 7182-2015 standard, except for water content and FFA (Kusumaningtyas et al., 2020). These results are possible because the water removal process's conditions (both temperature and time) are inappropriate (Ponnapa et al., 2016). Likewise, the FFA content is still relatively high because KSO as feedstock after the degumming process has a high FFA content (about 10%).

The FFA levels were still high in this investigation because the esterification and transesterification were carried out simultaneously under refluxed methanol to examine the synthesized ZnO/FA nanocomposite catalyst. From **Table 3**, it can be seen that the best biodiesel product characteristics are found in 50% NZO loading with the addition of NaOH according to stoichiometry, with a free fatty acid content of 2.6298%, saponification number 196, density 0.087713 gr/ml, viscosity 3.13 cSt, water content 0.005 and iodine number of 62.14 gr $I_2$/100 gr. Therefore, the FFA content of KSO must be at a low value before the transesterification process. Therefore, increasing KSOB and FFA content yield in KSOB products is expected to comply with SNI 7182-2015 standards.

**Table 3.** Comparison of KSOB properties with biodiesel standard according to SNI 7182-2015

| Parameter | *value* | SNI 7182-2015 |
|---|---|---|
| Density (gr/ml) | 0,87—0.89 | 0,85 - 0,89 |
| FFA as Linoleic (%w/w) | 2.55 | max. 0,6 |
| Iodine Value (gr $I_2$/100 g) | 63.78 | max. 115 |
| Moisture Content (%w/w) | 0.15 | max. 0.05 |
| Viscosity (cSt) | 2.6-3.2 | 2.3 – 6.0 |

## 4. Conclusions

Researchers successfully developed a fly ash-supported nano zinc oxide catalyst using a mix of techniques (coprecipitation, precipitation, and impregnation). The optimal catalyst, boasting a surface area of 14.29 m²/g, was achieved by precisely adding NaOH and loading it with 60% ZnO. This catalyst effectively converted low-quality kapok seed oil (10% FFA) into biodiesel, reaching a maximum yield of 64.29% under specific conditions (80°C, 1:15 oil-to-methanol ratio, 3% catalyst, 3 hours reaction time). The produced biodiesel met the national standard (SNI 7182-2015). These results highlight

the potential of this catalyst for low-grade oil conversion. Moreover, modifying the synthesis route by pre-treating and functionalizing the fly ash support with sulfonates holds promise for further enhancing the catalyst's effectiveness, and resulting in high biodiesel yield.

## Acknowledgments

We gratefully acknowledge the financial support of the Research and Community Services Institutions of Universitas Ciputra Surabaya. This research was made possible through the DIP-BIMA grant (contract number 007/UC-LPPM/DIP-BIMA/SP3H/IX/2023).

## References

AlSharifi, M., & Znad, H. (2019). Development of a lithium-based chicken bone (Li-Cb) composite as an efficient catalyst for biodiesel production. *Renewable Energy, 136*, 856–864. doi: 10.1016/j.renene.2019.01.052.

Asri, N. P., Machmudah, S., Wahyudiono, W., Suprapto, S., Budikarjono, K., Roesyadi, A., & Goto, M. (2013). Non-Catalytic Transesterification of Vegetables Oil to Biodiesel in Sub-and Supercritical Methanol: A Kinetic's Study. *Bulletin of Chemical Reaction Engineering & Catalysis* 7(3), 215–223. doi: 10.9767/bcrec.7.3.4060.215-223.

Asri, N. P., Machmudah, S., Wahyudiono, W., Suprapto, S., Budikarjono, K., & Roesyadi, A., Goto, M. (2013). Palm oil transesterification in sub- and supercritical methanol with heterogeneous base catalyst. *Chemical Engineering and Processing: Process Intensification 72*, 63–67. doi: 10.1016/j.cep.2013.07.003.

Asri, N. P., Prasetiyo, W. D., Kafidhu, A., Atiqoh, A., Puspitasari, E.A., Hindarso, H., & Suprapto, S. (2020). Transesterification of kapok seed oil (Ceiba pentandra) using heterogeneous catalyst bimetallic oxide of zinc and copper supported by γ-alumina. *Materials Science Forum, 988*, 87–94. doi: 10.4028/www.scientific.net/msf.988.87.

Asri, N. P., Saraswati, S., Yogaswara, R. R., Puspitasari, D. A, Mirzayanti, Y. W., & Udyani, K. (2021). Functionalization of Multiwall Carbon Nano-Tube Supported Zinc Oxide Solid Acid Catalyst Using Sulfonate Compound for Transesterification of Schleichera Oleosa L Oil. *Journal of Physics: Conference Series, 2117*(1). doi: 10.1088/1742-6596/2117/1/012038.

Asri, N. P., Saraswati, S., Hindarso, H., Mirzayanti, Y. W., & Yogaswara, R. R. (2021). Study of catalyst support utilization on ZnO-based solid catalyst to its activity at transesterification of Kesambi (Schleichera oleosa) oil. IOP Conference Series: *Materials Science and Engineering, 1034*(1). doi: 10.1088/1757-899x/1034/1/012059.

Asri, N. P., Yunati, Y., Hindarso, H., & Yogaswara, R. R. (2020). Preparation of Multi-Walled Carbon Nanotubes Supported Zinc Oxide Catalyst for Transesterification of Kesambi (Schleichera oleosa) Oil. IOP Conference Series: *Materials Science and Engineering, 742*(1). doi: 10.1088/1757-899X/742/1/012034.

Asri, N. P., Saraswati, R., Hindarso, H., Puspitasari, D. A., & Suprapto. 2021. Synthesis of biodiesel from kesambi (Schleichera oleosa L.) oil using carbon nanotube-supported zinc oxide heterogeneous catalyst. *IOP Conference Series: Earth and Environmental Science, 749*(1). doi: 10.1088/1755-1315/749/1/012048.

Asri, N. P., Soe'eib, S., Poedjojono, B., & Suprapto. 2018. Alumina supported zinc oxide catalyst for production of biodiesel from kesambi oil and optimization to achieve highest yields of biodiesel. *Euro-Mediterranean Journal for Environmental Integration, 3*(1), 3. doi: 10.1007/s41207-017-0043-8.

Asri, N. P., Yuniati, Y., Hindarso, H., Suprapto, & Yogaswara, R. R. 2020. Biodiesel production from Kesambi (Schleichera oleosa) oil using multi-walled carbon nanotubes supported zinc oxide as a solid acid catalyst. *IOP Conference Series: Earth and Environmental Science, 456*(1), 012003. doi: 10.1088/1755-1315/456/1/012003.

Asri, N. P., Budikarjono, K., & Roesyadi, A. 2015. Kinetics of Palm Oil Transesterification Using Double Promoted Catalyst CaO/KI/γ-$Al_2O_3$. *Journal of Engineering and Technological Sciences*, *47*(4), 353–363. doi: 10.5614/j.eng.technol.sci.2015.47.4.1.

Asri, N. P., Yuniati, Y., Hindarso, H., Suprapto, & Yogaswara, R. R. 2020. Transesterification of kapok seed oil (Ceiba pentandra) using heterogeneous catalyst bimetallic oxide of zinc and copper supported by γ-alumina. *Materials Science Forum, 988*, 87–94. doi: 10.4028/www.scientific.net/msf.988.87.

Babajide, O., Musyoka, N., Petrik, L., & Ameer, F. (2012). Novel zeolite Na-X synthesized from fly ash as a heterogeneous catalyst in biodiesel production. *Catalysis Today, 190*(1), 54–60. doi: 10.1016/j.cattod.2012.04.044.

Babajide, O., Petrik, L., Musyoka, N., Amigun, B., & Ameer, F. (2010). Application of coal fly ash as a solid basic catalyst in producing biodiesel. *AIChE Annual Meeting Conference Proceedings.*

Gurunathan, B., & Ravi, A. (2015). Biodiesel production from waste cooking oil using copper doped zinc oxide nanocomposite as heterogeneous catalyst. *Bioresource Technology, 188*, 124–127. doi: 10.1016/j.biortech.2015.01.012.

He, P. Y., Zhang, Y. J., Chen, H., Han, Z. C., & Liu, L. C. (2019). Low-energy synthesis of kaliophilite catalyst from circulating fluidized bed fly ash for biodiesel production. *Fuel, 257*, 116041. doi: 10.1016/j.fuel.2019.116041.

Helwani, Z., Ramli, M., Saputra, E., Putra, Y. L., Simbolon, D. F., Othman, M. R., & Idroes, R. (2020). Composite catalyst of palm mill fly ash-supported calcium oxide obtained from eggshells for transesterification of off-grade palm oil. *Catalysts, 10*(7). doi: 10.3390/catal10070724.

Istadi, I., Anggoro, D. D., Buchori, L., Rahmawati, D. A., & Intaningrum, D. (2015). Active Acid Catalyst of Sulphated Zinc Oxide for Transesterification of Soybean Oil with Methanol to Biodiesel. *Procedia Environmental Science, 23*, 385–393. doi: 10.1016/j.proenv.2015.01.055.

Katara, S., Kabra, S., Goyal, D., Hada, R., Sharma, A., & Rani, A. (2020). Fly ash to solid base catalyst: Synthesis, characterization and catalytic application. *Materials Today: Proceedings, 42*, 1409–1416. doi: 10.1016/j.matpr.2021.01.148.

Khan, T. M. Y. (2020). A Review of Performance-Enhancing Innovative Modifications in Biodiesel Engines. *Energies, 13*(17), 4395. doi: 10.3390/en13174395.

Kusumaningtyas, R. D., Utomo, M. Y. A., Nurjanah, P. R., & Widjanarko, D. 2020. Synthesis of biodiesel from kapok (Ceiba pentandra L.) seed oil through ultrasound-enhanced transesterification reaction. *AIP Conference Proceedings* 2217(1), 2–11. doi: 10.1063/5.0000609.

Malpani, S. K., & Rani, A. (2019). A Greener Route for Synthesis of Fly Ash Supported Heterogeneous Acid Catalyst. *Materials Today: Proceedings, 9*, 551–559. doi: 10.1016/j.matpr.2018.10.375.

Mandolesi de Araújo, C. D., de Andrade, C. C., de Souza e Silva, E., & Dupas, F. A. (2013). Biodiesel production from used cooking oil: A review. *Renewable and Sustainable Energy Reviews, 27*, 445–452. doi: 10.1016/j.rser.2013.06.014.

Mukenga, M. (2012). *Biodiesel production over supported Zinc Oxide nanoparticles*. University of Johannesburg.

Muñoz, R., Gonzales, A., Valdebenito, F., Ciudad, G., Navia, R., Pecchi, G., & Azocar, L. (2020). Fly ash as a new versatile acid-base catalyst for biodiesel production. *Renewable Energy, 162*, 1931–1939. doi: 10.1016/j.renene.2020.09.099.

Nair, P., Singh, B., Upadhyay, S., & Sharma, Y. C. (2012). Synthesis of biodiesel from low FFA waste frying oil using calcium oxide derived from mereterix as a heterogeneous catalyst. *Journal of Cleaner Production, 29–30*, 82–90. doi: 10.1016/j.jclepro.2012.01.039.

Olutoye, M. A., & Hameed, B. H. (2011). Synthesis of fatty acid methyl ester from used vegetable cooking oil by solid reusable $Mg_{1-x}Zn_{1+x}O_2$ catalyst. *Bioresource Technology, 102*(4), 3819–3826. doi: 10.1016/j.biortech.2010.11.100.

Perhutani. (2022). Optimalkan Pemanfaatan Hutan Dengan Budidaya Kapuk Randu, Perhutani Tandatangani Mou Bersama RWH. Retrieved from https://www.perhutani.co.id/optimalkan-pemanfaatan-hutan-dengan-budidaya-kapuk-randu-perhutani-tandatangani-mou-bersama-rwh/. Access April 8, 2022.

Ponappa, K., Velmurugan, V., Franco, P. A., Kannan, T. R., & Ragurajan, R. (2016). Optimization of Biodiesel Production from Ceiba Pentandra (Kapok Seed Oil) Using Response Surface Methodology Assisted by Ultrasonic Energy Method. *International Journal of Chemical Technology Research, 9*(5), 794–803.

Putri, E. M. M., Rachimoellah, M., Santoso, N., & Pradana, F. (2012). Biodiesel production from kapok seed oil (Ceiba pentandra) through the transesterification process by using CaO as catalyst. *Global Journal of Research in Engineering and Chemical Engineering, 12*(2), 6–11.

Risdanareni, P., Puspitasari, P., & Januarti Jaya, E. (2017). Chemical and Physical Characterization of Fly Ash as Geopolymer Material. *MATEC Web of Conferences, 97*. doi: 10.1051/matecconf/20179701031.

Roy, T., Sahani, S., & Sharma, Y. C. (2020). Green synthesis of biodiesel from Ricinus communis oil (castor seed oil) using potassium promoted lanthanum oxide catalyst: kinetic, thermodynamic and environmental studies. *Fuel, 274*, 117644. doi: 10.1016/j.fuel.2020.117644.

Sharma, Y. C., & Singh, B. (2010). A hybrid feedstock for a very efficient preparation of biodiesel. *Fuel Processing Technology*, *91*, 1267–1273. doi: 10.1016/j.fuproc.2010.04.008.

Sharma, Y. C., Singh, B., & Korstad, J. (2010). High Yield and Conversion of Biodiesel from a Nonedible Feedstock (Pongamia pinnata). *Journal of Agricultural and Food Chemistry, 58*(1), 242–247. doi: 10.1021/jf903227e.

Widjanarko, D., Kusumaningtyas, R. D., & Fathoni, A. A. (2020). Alteration of Biodiesel Properties and Automotive Diesel Engine Performance due to Temperature Variation of the Transesterification Process. *Jurnal Rekayasa Kimia dan Lingkungan, 15*(2) 90–98. doi: 10.23955/rkl.v15i2.16007.

Yusuff, A. S., Yusuff., A. S., Bhonsle, A. K., Trivedi, J., Bangwal, D. P., Singh, L. P., & Atray, N. (2021). Synthesis and characterization of coal fly ash supported zinc oxide catalyst for biodiesel production using used cooking oil as feed. *Renewable Energy, 170*, 302–314. doi: 10.1016/j.renene.2021.01.101.

Yusuff, A. S., & Bello, K. A. (2019). Synthesis of fatty acid methyl ester via transesterification of waste frying oil by a zinc-modified pumice catalyst: Taguchi approach to parametric optimization. *Reaction Kinetics, Mechanisms and Catalysis 128*(2), 739–761. doi: 10.1007/s111